the plant journal

SEB SOCIETY FOR EXPERIMENTAL BIOLOGY

The Plant Journal (2022) doi: 10.1111/tpj.15671

Expression of *Chlamydomonas reinhardtii* chloroplast diacylglycerol acyltransferase 3 is induced by light in concert with triacylglycerol accumulation

María de las Mercedes Carro[1,†,‡], Gabriela Gonorazky[1,†], Débora Soto[1], Leandro Mamone[1,§], Carolina Bagnato[2], Luciana A. Pagnussat[3] and María Verónica Beligni[1,*]

[1]*Instituto de Investigaciones Biológicas (IIB-CONICET-UNMdP), Facultad de Ciencias Exactas y Naturales, Universidad Nacional de Mar del Plata, B7608FBY, Mar del Plata, Argentina,*

[2]*Instituto de Energía y Desarrollo Sustentable (IEDS), Comisión Nacional de Energía Atómica, Centro Atómico Bariloche, 8400, San Carlos de Bariloche, Argentina, and*

[3]*Facultad de Ciencias Agrarias, Universidad Nacional de Mar del Plata, B7620EMA, Balcarce, Argentina*

Received 19 January 2021; revised 15 December 2021; accepted 9 January 2022

*For correspondence (e-mail mvbeligni@mdp.edu.ar).

[†]These authors contributed equally to this work.

[‡]Present address: Department of Biomedical Sciences and Center for Reproductive Genomics, Cornell University, Ithaca, NY, 14853, USA

[§]Present address: Centro de Investigaciones sobre Porfirinas y Porfirias (CIPYP), CONICET and Hospital de Clínicas José de San Martín, Universidad de Buenos Aires, 1120AAF, Ciudad de Buenos Aires, Argentina

SUMMARY

Considerable progress has been made towards the understanding of triacylglycerol (TAG) accumulation in algae. One key aspect is finding conditions that trigger TAG production without reducing cell division. Previously, we identified a soluble diacylglycerol acyltransferase (DGAT), related to plant DGAT3, with heterologous DGAT activity. In this work, we demonstrate that *Chlamydomonas reinhardtii* DGAT3 localizes to the chloroplast and that its expression is induced by light, in correspondence with TAG accumulation. *Dgat3* mRNAs and TAGs increase in both wild-type and starch-deficient cells grown with acetate upon transferring them from dark or low light to higher light levels, albeit affected by the particularities of each strain. The response of *dgat3* mRNAs and TAGs to light depends on the pre-existing levels of TAGs, suggesting the existence of a negative regulatory loop in the synthesis pathway, although an effect of TAG turnover cannot be ruled out. Altogether, these results hint towards a possible role of DGAT3 in light-dependent TAG accumulation in *C. reinhardtii*.

Keywords: *Chlamydomonas*, chloroplast, diacylglycerol acyltransferase, light response, triacylglycerols.

INTRODUCTION

Current interest in the development of sustainable sources of liquid fuels and other industrial compounds has driven a remarkable expansion in the study of eukaryotic microalgae as feedstock for triacylglycerols (TAGs) (Banerjee *et al.*, 2016; Li-Beisson *et al.*, 2019; Sato *et al.*, 2017; Xu *et al.*, 2016). One of the most remarkable contributions to this field was the finding that neutral lipid generation in algae could be induced by stress and nutrient depletion (Allen *et al.*, 2018; Pal *et al.*, 2011; Rearte *et al.*, 2018; Sharma *et al.*, 2012; Yang *et al.*, 2015). The best-characterized condition is nitrogen deprivation, which stimulates TAG production in the majority of the algal species studied, independently of their taxonomic classification and lifestyles (Blaby *et al.*, 2013; Martin *et al.*, 2014; Msanne *et al.*, 2012; Weng *et al.*, 2014). Likewise, most of the enzymes investigated to date that participate in TAG synthesis are those that respond to a lack of nitrogen (Banerjee *et al.*, 2017; Boyle *et al.*, 2012; Chen *et al.*, 2015; Guo *et al.*, 2017; Xu *et al.*, 2018). These enzymes are mostly homologs of proteins characterized in animals, yeast and plants that are involved in the conventional pathway carried out in the endoplasmic reticulum (ER)/cytosol (Bhatt-Wessel *et al.*, 2018; Liu *et al.*, 2011; Lung & Weselake, 2006; Shockey *et al.*, 2006). Despite these advances, the drawback of any production scheme based on nitrogen deprivation is that TAG accumulation occurs in parallel with a decrease in algal cell division, which reduces the total lipid productivity (Takeuchi & Benning, 2019). Hence, finding conditions that yield large quantities of TAGs

during optimal growth is one of the big conundrums in this research area.

With this challenge in mind, we set out to search for novel enzymes that could participate in TAG synthesis in algae of diverse evolutionary origins. Using a HMMER iterative approach (Bagnato *et al.*, 2017a), we identified a soluble diacylglycerol acyltransferase (DGAT) exclusive to green algae and moderately related to plant DGAT3 (Bagnato *et al.*, 2017b). DGATs catalyze the formation of TAG by performing an acylation of a fatty acid (FA), most frequently activated as an acyl-CoA, onto the sn-3 position of a molecule of diacylglycerol (DAG) (Yen *et al.*, 2008). Phylogenetic analysis showed that the DGAT3 clade shares a most recent ancestor with a group of uncharacterized proteins from cyanobacteria, suggesting a prokaryotic origin, whereas the canonical DGATs, DGAT1 and DGAT2, are only related to proteins from eukaryotes. In addition, most of the algal sequences within the DGAT3 group have predicted chloroplast localization (Bagnato *et al.*, 2017b). In plants, DGAT3 has been characterized in only a few species, including *Arabidopsis thaliana*, *Arachis hypogaea* (peanut) and *Vernicia fordii* (tung tree) (Aymé *et al.*, 2018; Cao *et al.*, 2013; Chi *et al.*, 2014; Hernández *et al.*, 2012; Saha *et al.*, 2006). DGAT3 protein sequences show very distinctive features, particularly in comparison with DGAT1 and DGAT2 (Cao, 2011; Liu *et al.*, 2012; Turchetto-Zolet *et al.*, 2011). The most conspicuous difference between DGAT3 and its counterparts is the fact that its sequence exhibits a carboxy terminal iron–sulfur (2Fe–2S) cluster-binding domain that has a fold similar to that present in thioredoxins (Aymé *et al.*, 2018; Bagnato *et al.*, 2017b). Although the role of this domain in DGAT3 remains unknown, the majority of the homologs that have been studied to date act as low-potential electron carriers (Fukuyama, 2004; Zu *et al.*, 2002).

The acylation activities of DGAT1 and DGAT2 have been widely described and reviewed (Yen *et al.*, 2008). The conserved amino acids of these two protein families have been extensively studied in animals, yeast and plants, and some of the residues that are important for catalysis have been determined in mutagenesis experiments (Liu *et al.*, 2011; Lopes *et al.*, 2014; Stone *et al.*, 2006). In contrast, DGAT3 activity has only been demonstrated *in vitro* for the *Arabidopsis thaliana*, *Arachis hypogaea* and *Chlamydomonas reinhardtii* proteins (Aymé *et al.*, 2018; Bagnato *et al.*, 2017b; Chi *et al.*, 2014; Hernández *et al.*, 2012; Saha *et al.*, 2006), and little is known about the identity or location of the acylation domains. We previously reported that *C. reinhardtii* DGAT3 expressed in *Escherichia coli* produced an increase in TAGs in the presence of oleate (Bagnato *et al.*, 2017b). In the DGAT3 protein sequence, we identified three histidine-containing motifs similar to those that perform acylation in glycerol-3-phosphate acyltransferase (GPAT) and acylglycerol-3-phosphate acyltransferase (AGPAT) (Takeuchi & Reue, 2009; Yamashita *et al.*, 2014), but those motifs have not been functionally analyzed.

The content of hydrophobic regions in DGAT3 is considerably lower than those of DGAT1 and DGAT2. Additionally, many of the hydrophobic regions of the latter two proteins translate into transmembrane segments, whereas DGAT3 appears to have no transmembrane domains. Most remarkably, in DGAT1 and DGAT2, the catalytic motifs either flank or are partially embedded in hydrophobic regions, whereas the putative catalytic motifs of *C. reinhardtii* DGAT3 are flanked by hydrophilic regions. All these observations led us to hypothesize that DGAT3 participates in a soluble TAG synthesis pathway in the chloroplast, where it could act as an electron carrier in addition to performing an acylation reaction (Bagnato *et al.*, 2017b).

In this work, we demonstrate empirically that *C. reinhardtii* DGAT3 is targeted to the chloroplast and advance our knowledge of its metabolic regulation. We demonstrate that DGAT3 expression is induced by light in the presence of acetate in two different strains and that this induction occurs in correspondence with light-dependent TAG accumulation. Both DGAT3 expression and TAG levels increase upon shifting cells from dark or low light levels to higher light levels, albeit affected by the particularities of each strain. Altogether, our results suggest that light-dependent TAG accumulation could be carried out, at least in part, by the action of DGAT3. In addition, our results further interrogate the relationship between light and carbon with regards to TAG metabolism.

RESULTS

Figure 1(a) shows a schematic representation of the *C. reinhardtii* DGAT3 full-length protein. This polypeptide has a transit peptide of approximately 70 amino acids, as predicted by both PREDALGO and TARGETP (Bagnato *et al.*, 2017b). Contiguous to this fragment, the sequence features a region of about 223 amino acids with no apparent structure. In this disordered portion, we previously predicted at least two putative acyltransferase motifs that include the conserved histidine that most frequently acts as catalytic residue (Bagnato *et al.*, 2017b). To the carboxy end, DGAT3 has a conserved 2Fe–2S cluster-binding domain, which we previously modeled on the thioredoxin-like ferredoxin of *Aquifex aeolicus* (Yeh *et al.*, 2000), followed by a carboxy end with no significant similarity to any characterized motif.

In order to confirm the chloroplast targeting prediction, we performed the immunolocalization of DGAT3 and subcellular fractionation followed by Western blot analysis. For immunolocalization, the characteristic anatomy and polarity of *C. reinhardtii* cells help researchers to locate fluorescence signals in particular subcellular areas. The single chloroplast has a cup-shaped appearance, with a main

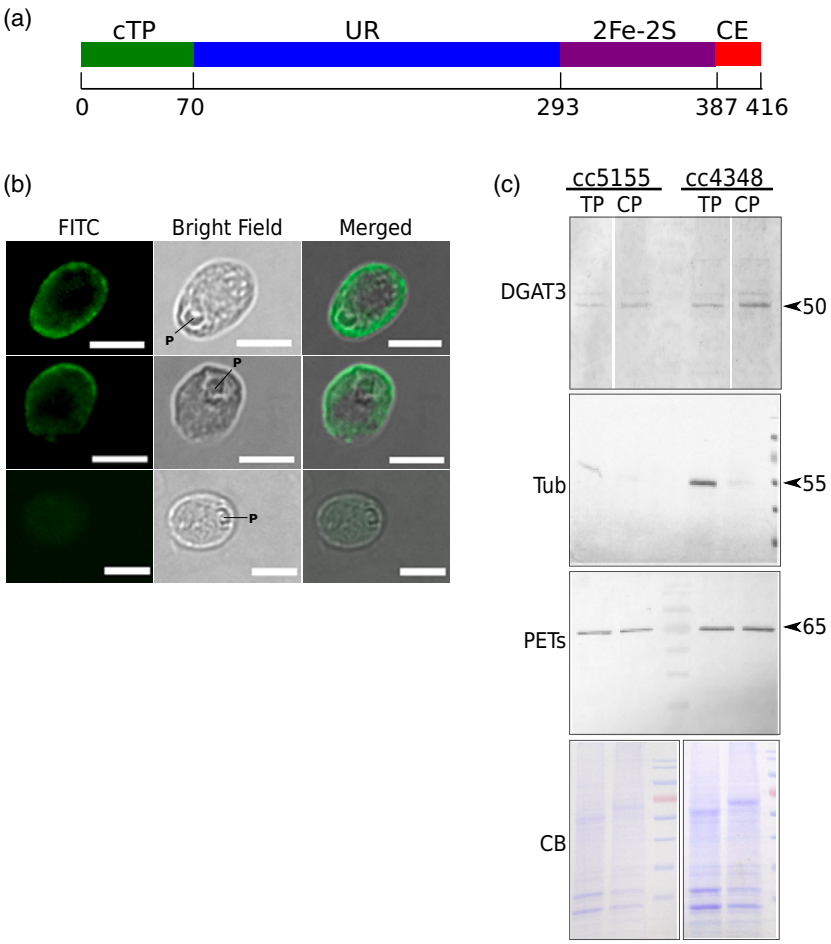

Figure 1. *Chlamydomonas reinhardtii* DGAT3 localizes to the chloroplast. (a) Schematic representation of the DGAT3 protein showing the predicted chloroplast transit peptide (cTP), the amino terminal unstructured region (UR), the 2Fe–2S cluster-binding domain (2Fe–2S) and the non-homologous carboxy end (CE). The numbers below are the predicted amino acid positions of each domain junction. (b) Representative images of immunofluorescent *C. reinhardtii* cells (cc-5155 strain) stained with either anti-DGAT3 primary antibodies plus FITC-conjugated secondary antibodies (top and middle panels) or cells stained with FITC-conjugated secondary antibodies only (lower panel). The left panels show green fluorescence, the middle panels show bright-field images of the same cells and the right panels show the previous two images merged, with the fluorescence signal increased for a better visualization of fluorescence localization. P, pyrenoid. Scale bars: 5 μm. (c) Western blot analysis of total protein (TP) and chloroplast protein (CP) fractions from *C. reinhardtii* strains cc-5155 and cc-4348. Proteins were separated in 12% SDS-polyacrylamide gels and either stained with Coomassie Brilliant Blue (CB, 5 μg protein per lane) or analyzed by Western blot using anti-DGAT3 (10 μg), anti-tubulin (Tub, 5 μg) and anti-PETs (5 μg) antibodies. Arrowheads indicate approximate molecular weights in kDa, estimated by comparison with molecular size standards.

posterior globular domain from which finger-like lobes extend to the apical pole and surround the main portion of the cytosol and nucleus (Uniacke *et al.*, 2011). Near the posterior pole, the pyrenoid is one of the most conspicuous structures. Figure 1(b) shows that green fluorescence was consistent with chloroplast localization when *C. reinhardtii* cc-5155 cells were treated with anti-DGAT3 primary antibodies followed by fluorescein isothiocyanate (FITC)-conjugated secondary antibodies (top and middle panels), whereas fluorescence was negligible in cells treated with FITC-conjugated antibodies alone (negative control, bottom panel). DGAT3 fluorescence was slightly non-homogeneous, with several spots of higher intensity and an uneven distribution in the pyrenoid (Figure 1b).

For the second strategy, we isolated *C. reinhardtii* chloroplasts from two cell wall-less strains, cc-5155 and cc-4348 (*sta6*), and analyzed the presence of DGAT3 by Western blot analysis. Figure 1(c) shows that the DGAT3 protein was present to similar levels in both total protein and chloroplast protein samples from both strains. As expected, the chloroplast polyprotein of elongation factor Ts (PETs) (Beligni *et al.*, 2004) was also detected similarly in both fractions, whereas only traces of β-tubulin, a cytosolic marker, were observed in chloroplast fractions. These results indicate that the isolated chloroplasts contained only a small level of contamination from whole cells and that *C. reinhardtii* DGAT3 is present in the chloroplast. Altogether, our results indicate that *C. reinhardtii* DGAT3 is indeed a chloroplast protein.

All proteins containing 2Fe–2S cluster-binding domains characterized so far act as low-potential electron carriers (Fukuyama, 2004; Zu *et al.*, 2002). This prompted us to hypothesize that DGAT3 might accomplish the synthesis of TAGs in conjunction with the photosynthetic machinery, and hence respond to light. TAGs were previously shown to increase in *C. reinhardtii* cc-124 cells after transferring them from low light to saturating light (Goold *et al.*, 2016), but the enzymes responsible for this accumulation remain unknown. With the purpose of evaluating whether DGAT3 participated in this response, we cultured cc-125 wild-type cells in Tris-acetate-phosphate (TAP) media under continuous light of 50 μmol photon m^{-2} sec^{-1} until they reached a cell density of 3×10^6 cells ml^{-1}, transferred them to low light (20 μmol photon m^{-2} sec^{-1}) for 16 h and then shifted them to high light (200 μmol photon m^{-2} sec^{-1}). Expression was determined by reverse transcription

quantitative polymerase chain reaction (RT-qPCR). Two genes were evaluated as potential endogenous controls: *actin* and *gblp*. According to RT-qPCR data, *gblp* levels were stable in the experiments tested (Tables S1 and S2), whereas *actin* fluctuated considerably upon transferring cc-125 cells from dark to light (data not shown). By virtue of these results, the expression levels of all target genes were subsequently normalized to *gblp* levels.

Figure 2(a) shows that *dgat3* mRNAs increased 1 h after transferring the cells to high light, peaked at 6 h into the high-light period (approximately 5.0-fold) and declined at longer times, remaining at about 2.5-fold until the end of the experiment. Figure 2(b,c) shows that, in the same conditions, TAGs also increased at 1 h into the high-light period and reached a maximum at 6 h (approximately 13.0-fold increase compared with the sample at the end of the dark period), decreasing to almost basal levels afterwards.

To determine the response to light of other enzymes that perform TAG synthesis, we analyzed the mRNA levels of DGAT1 and phospholipid:diacylglycerol acyltransferase (PDAT). We selected those two enzymes because both have the potential to carry out TAG synthesis in the chloroplast, according to previous evidence (Bagnato *et al.*, 2017b; Yoon *et al.*, 2012). Quality control of RT-qPCR data indicated that the results obtained for *dgat1* mRNAs were sound. In contrast, for cc-125 cells, the cycle threshold counts (Cts) of *pdat* mRNAs were very high and the melting curves contained multiple peaks, making the analysis unreliable (data not shown). Thus, only *dgat3* and *dgat1* mRNA levels are reported for the cc-125 strain. In the experiment presented in Figure 2(a), *dgat1* mRNAs showed a moderate but steady increase of approximately 2.0-fold between 1 and 12 h into the high-light period, decreasing again to the initial levels at the end of the experiment. These results suggest that DGAT3 and DGAT1 could participate in TAG synthesis when transferring wild-type cells from low light to high light.

In addition to investigating possible enzymatic components of TAG accumulation under saturating light, we wished to evaluate whether the increase in TAGs also happened at non-saturating light intensities. For that purpose, we performed classical light-activation experiments by studying the effect of shifting wild-type cells from dark to moderate light (Beligni *et al.*, 2004; Coragliotti *et al.*, 2011). The cc-125 cells were cultured under continuous light of 50 μmol photon m^{-2} sec^{-1} until they reached a cell density

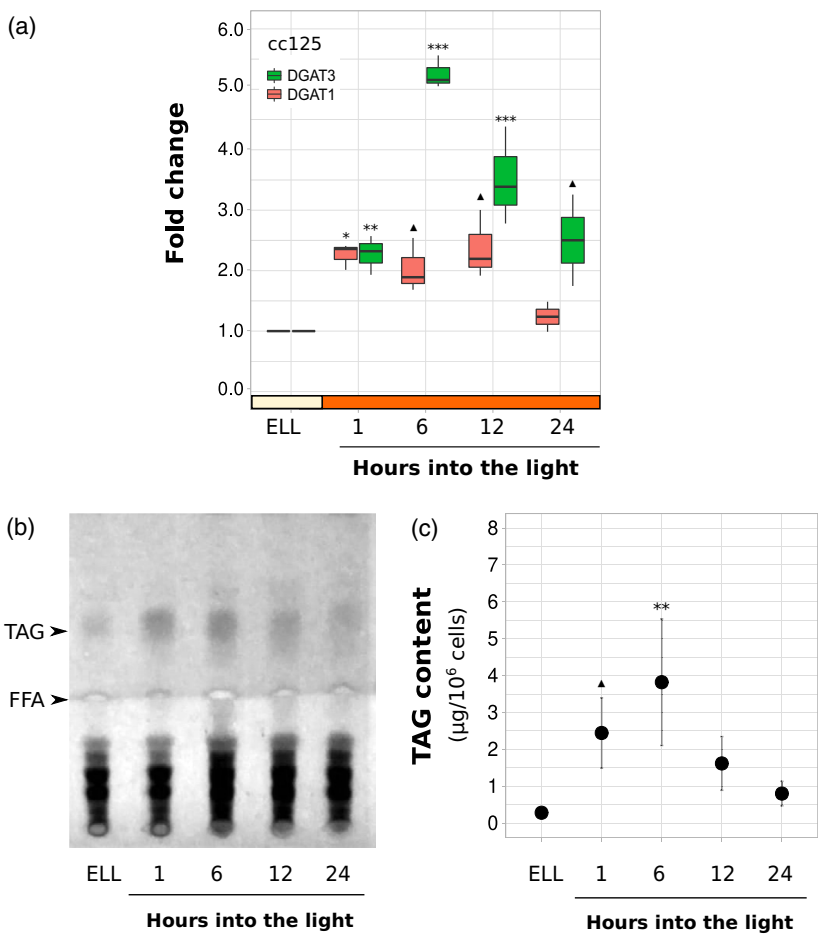

Figure 2. *dgat3* mRNAs and TAGs accumulate in the wild-type strain after shifting cells from low light to high light. Cells from the cc-125 strain were grown in TAP media under continuous light (50 μmol photons m^{-2} sec^{-1}) to approximately 3×10^6 cells ml^{-1}, transferred to 20 μmol photons m^{-2} sec^{-1} (low light period) for 16 h and then switched to 200 μmol photons m^{-2} sec^{-1} (high light) for 24 h. Samples were harvested at the end of the low light period (ELL) and at 1, 6, 12 and 24 h after shifting the cells to high light. (a) Box plots show the expression of *dgat3* and *dgat1* mRNAs analyzed by RT-qPCR. Results are expressed as the fold change of each gene in each condition compared with the endogenous control (*gblp*) in the same condition and compared with the ELL sample. Vertical bars indicate minimum and maximum values, horizontal black strips indicate median values. The pale yellow box represents the low-light period, the orange box represents the high-light period. (b) Total lipids were extracted from each sample and analyzed by thin layer chromatography (TLC). Sample volumes equivalent to 10 million cells were loaded in each lane. Arrowheads show the spots of triglyceride (TAG) and free fatty acid (FFA) standards. A representative image of three independent biological replicates is shown. (c) TAGs eluted from the spots in (b) were quantified using a colorimetric assay. Dots indicate average values; bars show standard deviations. Statistical analyses were performed by means of a one-way ANOVA and Dunnett's multiple-comparisons test. Significant differences of samples against the ELL sample are shown: ***$P < 0.001$, **$P < 0.01$, *$P < 0.05$, ▲$P < 0.1$.

of 3 × 10^6 cells ml^{-1}, then transferred to the dark for 16 h and then shifted back to the initial light conditions.

Figure 3(a) shows that no significant variations in *dgat3* or *dgat1* mRNAs were observed between the end of the dark period and the light period in cc-125 cells (Figure 3a; Table S3). In the same assays, no remarkable variations in TAG content occurred during the first 1 h of light compared with the end of the dark period, and a significant decline could be observed at longer times (Figure 3b,c; Table S3).

During photosynthetic growth, light provides the means to generate reducing power that needs to be harnessed properly in order to protect the photosystems. Thus, we hypothesized that it was possible to achieve an increase in TAG levels in wild-type cells by increasing the light intensity, in order to subject the cells to a condition in which the excess of reducing power could not be effectively stored solely in starch. To this end, we measured mRNA levels and TAG accumulation in cc-125 cells that were cultured in TAP media at 50 μmol photon m^{-2} sec^{-1} until they reached a cell density of 3 × 10^6 cells ml^{-1}, then transferred to the dark for 16 h before being moved into high light (200 μmol photon m^{-2} sec^{-1}). Figure 4(a) shows that, unexpectedly, *dgat3* mRNAs declined upon transferring cc-125 cells from dark to high light, whereas *dgat1* mRNA levels remained relatively stable. In the same conditions, TAGs remained relatively stable for the first 6 h, and declined at 12 and 24 h under high light (Figure 4b,c; Table S3).

When analyzing TAG content at the end of the dark period, we observed that the levels of these lipids were quite high in both moderate light and high light experiments (Figures 3c and 4c, respectively). In fact, the main difference between the responses observed in Figures 2 and 4, where the end light intensity remained the same, was the levels of TAGs before the light period, i.e. at either the end of the dark period (ED) or at the end of the low light period (ELL). As the levels of TAGs after prolonged periods at either 50 or 200 μmol photon m^{-2} sec^{-1} were relatively low (Figures 2c, 3c and 4c, after 24 h of light), we assumed that the high levels of TAGs at the ED originated from accumulation in the dark, probably through a reduction of O_2 in non-aerated batch cultures, as reported previously (Hemschemeier *et al.*, 2013). In agreement with this assumption, we observed that TAG levels increased during a 48 h period of dark and decreased slowly during the subsequent light period in cc-125 cells (Figure S1). Altogether, these results suggest that an increase in DGAT3 expression and TAG levels in response to light occurs in the cc-125 strain only when the pre-existing levels of TAGs are very low.

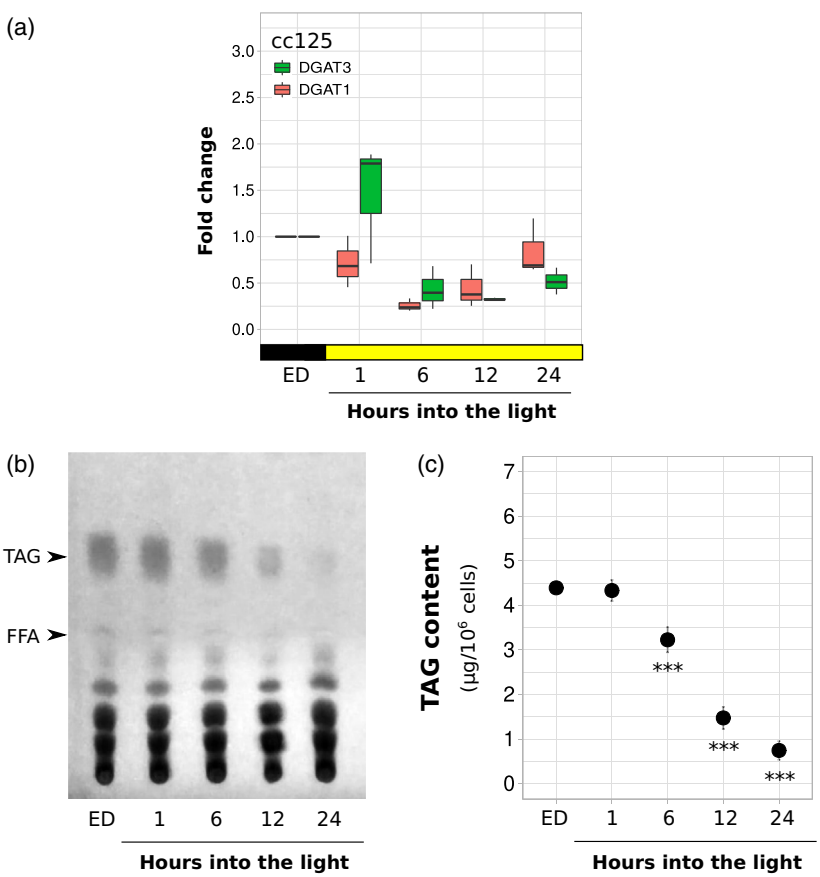

Figure 3. Response of *dgat3* mRNAs and TAGs after shifting wild-type cells from darkness to moderate light. *Chlamydomonas reinhardtii* cc-125 cells were grown in TAP media under continuous light (50 μmol photons m^{-2} sec^{-1}) to approximately 3 × 10^6 cells ml^{-1}, transferred to dark conditions for 16 h and were then transferred back to the initial light condition (moderate light). Samples were harvested at the end of the dark period (ED) and at 1, 6, 12 and 24 h after shifting the cells to light. (a) Box plots show the expression of *dgat3* and *dgat1* mRNAs analyzed by RT-qPCR. Results are shown as the fold change of each gene normalized to the endogenous control (*gblp*) in the same condition and to the ED sample. Values for independent biological triplicates are shown: vertical bars indicate minimum and maximum values; horizontal black strips indicate median values. The black box represents the dark period, the yellow box represents moderate light. (b) Total lipids were extracted from each sample and analyzed by TLC. Sample volumes equivalent to 20 million cells were loaded on each lane. Arrowheads show the spots of triglyceride (TAG) and free fatty acid (FFA) standards. A representative image of three independent biological replicates is shown. (c) TAGs eluted from the spots on (b) were quantified using a colorimetric assay. Dots indicate average values; bars show standard deviations. Statistical analyses were performed by means of a one-way ANOVA and Dunnett's multiple-comparisons test. Significant differences of samples against the ED sample are shown: ***$P < 0.001$.

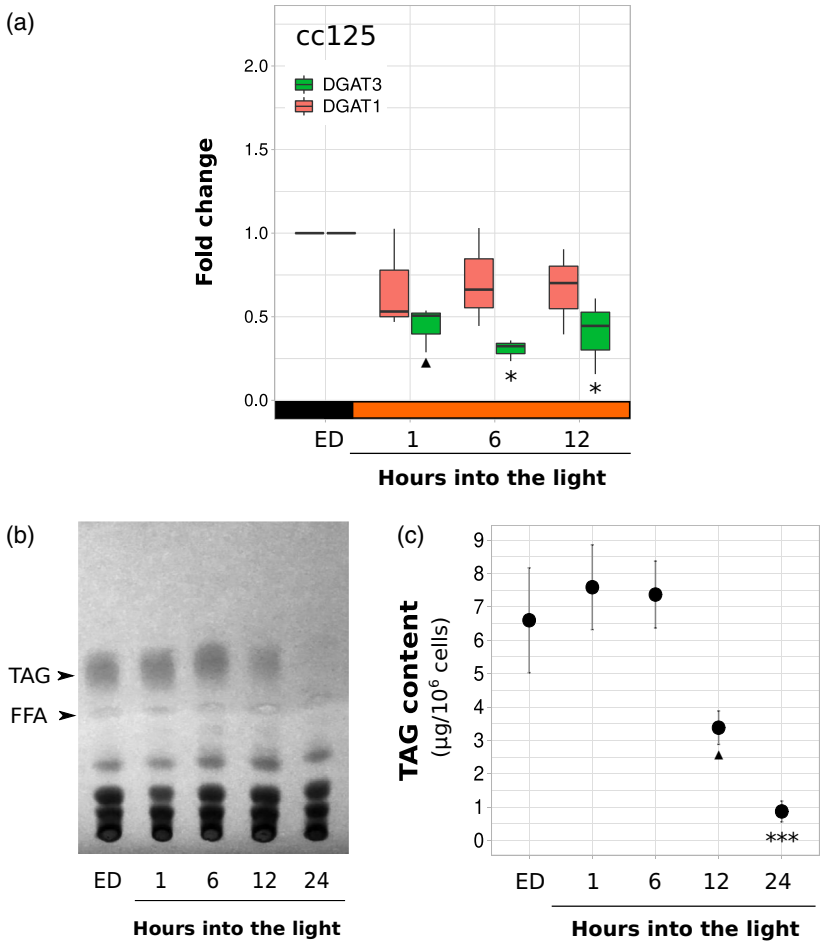

Figure 4. *dgat3* mRNAs and TAGs decrease in the wild-type strain after shifting cells from darkness to high light. Cells from cc-125 were grown in TAP media under continuous light (50 µmol photons m^{-2} sec^{-1}) to approximately 3×10^6 cells ml^{-1}, transferred to dark conditions for 16 h and then shifted to 200 µmol photons m^{-2} sec^{-1} (high light). Samples were harvested at the end of the dark period (ED) and at 1, 6, 12 and 24 h after shifting cells to light. (a) Box plots show the expression of *dgat3* and *dgat1* mRNAs analyzed by RT-qPCR. Results are expressed as the fold change of each gene normalized to the endogenous control (*gblp*) in the same condition and to the ED sample. Values for independent biological triplicates are shown: vertical bars indicate minimum and maximum values; horizontal black strips indicate median values. The black box represents the dark period; the orange box represents high light. (b) Total lipids were extracted from each sample and analyzed by TLC. Sample volumes equivalent to 20 million cells were loaded on each lane. Arrowheads show the spots of triglyceride (TAG) and free fatty acid (FFA) standards. A representative image of three independent biological replicates is shown. (c) TAGs eluted from the spots on (b) were quantified using a colorimetric assay. Dots indicate average values; bars show standard deviations. Statistical analyses were performed by means of one-way ANOVA and Dunnett's multiple-comparisons test. Significant differences of samples against the ED sample are shown: ***$P < 0.001$, *$P < 0.05$, ▲$P < 0.1$.

In view of the previous results, we hypothesized that the response to light would be different if TAGs were the only possible carbon storage metabolite. In order to evaluate this idea, we determined TAG and mRNA levels in cc-4348, a strain that has a deletion in the *STA6* gene (encoding a subunit of ADP-glucose pyrophosphorylase), which renders this strain deficient in starch synthesis (Zabawinski *et al.*, 2001). Although our objective was not to compare the results of this strain directly with those of the cc-125 wild-type strain, preliminary *dgat3* RT-qPCR results showed that the cell wall-less cc-5155 strain behaved similarly to the cc-125 strain when shifted from darkness to moderate light (Figure S2), which suggests that the absence/presence of the cell wall does not significantly affect the *dgat3* response to moderate light.

The cc-4348 cells were cultured under continuous light of 50 µmol photon m^{-2} sec^{-1} until a cell density of 3×10^6 cells ml^{-1} was reached, then transferred to the dark for 16 h and then shifted back to the initial light conditions, similarly to the experiment presented in Figure 3. Figure 5(a) shows that, in this strain, *dgat3* mRNAs increased 2.0-fold as early as 1 h into the light period, peaked at about 12 h (an average value of about 4.0-fold) and remained elevated until the end of the experiment (3.0-fold). In the same conditions, TAGs accumulated upon transferring the cells to moderate light, reaching a maximum after 6 h of the light period (a 4.4-fold increase compared with ED), and decreasing considerably at 24 h (Figure 5b,c; Table S3).

In cc-4348 cells, RT-qPCR analyses were reliable for both *dgat1* and *pdat* mRNAs. For this strain, although the high Cts obtained suggested that the levels of *pdat* mRNAs were very low, the melting curves and agarose gels obtained showed a single, pure amplicon (Tables S1 and S2). Figure 5(a) shows that both *dgat1* and *pdat* mRNAs decreased moderately in TAP-grown cc-4348 cells 1 h after shifting the cells from dark to moderate light conditions, and returned to the initial levels at 6–24 h under light. These results suggest that although TAG accumulation induced in cc-4348 cells by moderate light agrees with an increase in *dgat3* mRNAs, this accumulation cannot be explained by the pattern of *dgat1* and *pdat* mRNAs in our experimental conditions.

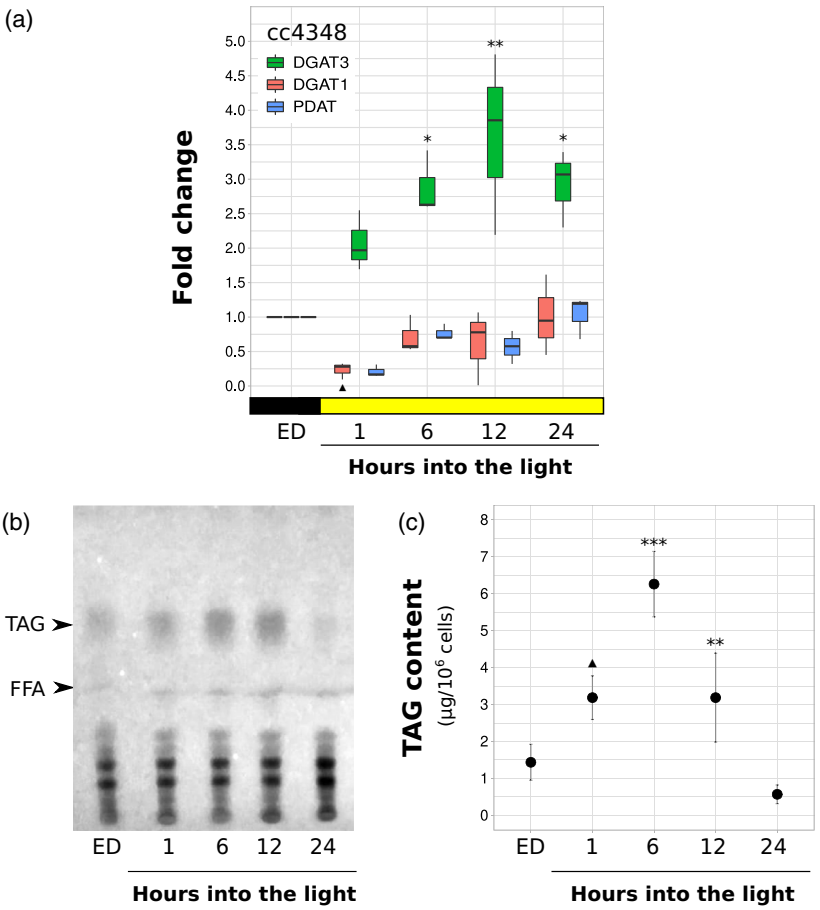

Figure 5. Exposure to moderate light triggers the accumulation of *dgat3* mRNAs and TAGs in *sta6* cells in the presence of acetate. *Chlamydomonas reinhardtii sta6* cells (cc-4348) were grown in TAP media under continuous light (50 µmol photons m^{-2} sec^{-1}) to approximately 3×10^6 cells ml^{-1}, transferred to dark conditions for 16 h and were then transferred back to the initial light condition (moderate light). Samples were harvested at the end of the dark period (ED) and at 1, 6, 12 and 24 h after shifting the cells to light. (a) Box plots showing the expression of *dgat3, dgat1* and *pdat* mRNAs analyzed by RT-qPCR. Results are shown as the fold change of each gene normalized to the endogenous control (*gblp*) in the same condition and to the ED sample. Values for independent biological triplicates are shown: vertical bars indicate minimum and maximum values; horizontal black strips indicate median values. The black box represents the dark period; the yellow box represents moderate light. (b) Total lipids were extracted from each sample and analyzed by TLC. Sample volumes equivalent to 10 million cells were loaded on each lane. Arrowheads show the spots of triglyceride (TAG) and free fatty acid (FFA) standards. A representative image of three independent biological replicates is shown. (c) TAGs eluted from the spots on (b) were quantified using a colorimetric assay. Dots indicate average values; bars show standard deviations. Statistical analyses were performed by means of one-way ANOVA and Dunnett's multiple-comparisons test. Significant differences of samples against the ED sample are shown: ***$P < 0.001$, **$P < 0.01$, *$P < 0.05$, ▲$P < 0.1$.

The accumulation of TAGs in the chloroplast has been reported to occur only in the presence of acetate (Fan *et al.*, 2011; Goodenough *et al.*, 2014; Goodson *et al.*, 2011). With the aim of analyzing if this pattern also held true for DGAT3 induction in cc-4348 cells, we analyzed *dgat3* mRNAs and TAG accumulation in this strain cultured in minimal media (without acetate) and transferred from dark to light, as in the previous experiment. Figure 6(a) shows that *dgat3* mRNAs were reduced significantly upon transferring the cells from dark to light in minimal media. In the same conditions, TAG content remained relatively stable for the first 12 h of the light period, undergoing a significant decrease at 24 h under light (Figure 6b,c; Table S3). Hence, we concluded that both light-induced DGAT3 expression and TAG accumulation depend upon the presence of acetate in the media in cc-4348 cells.

DISCUSSION

In this work, we report that light-induced TAG accumulation in *C. reinhardtii* occurs in agreement with the expression of DGAT3, a soluble, chloroplast-localized DGAT. In the conditions investigated, TAG production could not be fully explained by changes in the expression of DGAT1 or PDAT, two enzymes that could potentially synthesize TAGs on the chloroplast envelope. These results point to DGAT3 as a feasible and exciting candidate for light-induced TAG synthesis in the chloroplast, as shown in our proposed model (Figure 7).

In algae, TAG accumulation is mostly associated with the canonical ER/cytosol pathway (Tsai *et al.*, 2015; Weng *et al.*, 2014). However, under certain conditions, TAGs have also been proposed to accumulate in association with the chloroplast (Fan *et al.*, 2011; Goodson *et al.*, 2011). Goold *et al.* (2016) reported that saturating light triggers TAG synthesis in *C. reinhardtii*, both inside and outside the plastid, mostly associated with the chloroplast envelop. In this work, we report that DGAT3 expression and TAG accumulation do not only respond to high light but also undergo light-dependent induction in a broad sense, as their levels also increase at moderate light intensities, as proposed in the model of Figure 7(a). True light responses are expected to operate to some extent at all light intensities, including limiting light conditions, in which the rate of light absorption is well matched with the rate of photosynthesis (Björkman & Demmig, 1987). In our case, an increment in the content of TAGs after the transition from dark

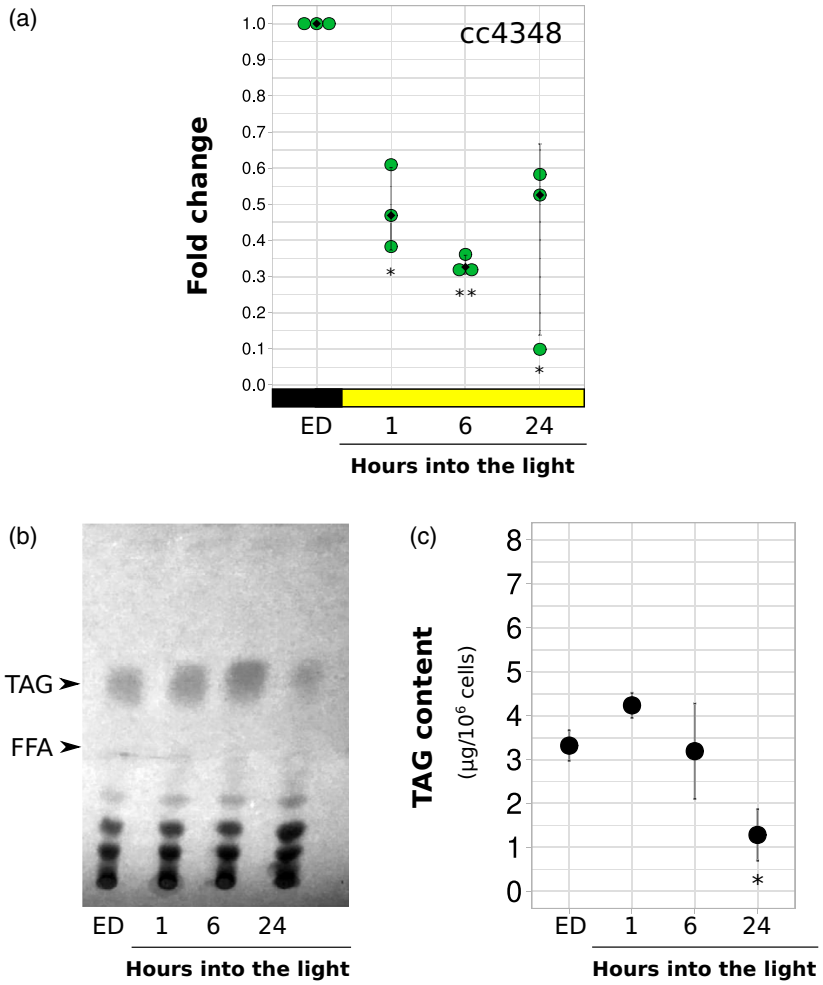

Figure 6. Response of *dgat3* mRNAs and TAGs to light in *sta6* cells grown in minimal media. Cells from the *sta6* mutant (cc-4348) were grown in Tris-minimal media under continuous light (50 μmol photons m^{-2} sec^{-1}) to approximately 3 × 10^6 cells ml^{-1}, transferred to dark conditions for 16 h and then transferred back to the initial light condition (moderate light). Samples were harvested at the end of the dark period (ED) and at 1, 6 and 24 h after shifting the cells to light. (a) Dot plot showing the expression of *dgat3* mRNAs analyzed by RT-qPCR. Results are expressed as the fold change of *dgat3* normalized to the endogenous control (*gblp*) in the same condition and to the ED sample. Green circular dots show the values of independent biological replicates. Vertical bars indicate standard deviations; black diamond dots show median values. The black box represents the dark period; the yellow box represents moderate light. (b) Total lipids were extracted from each sample and analyzed by TLC. Sample volumes equivalent to 20 million cells were loaded on each lane. Arrowheads show the spots of triglyceride (TAG) and free fatty acid (FFA) standards. A representative image of three independent biological replicates is shown. (c) TAGs eluted from the spots on (b) were quantified using a colorimetric assay. Dots indicate average values; bars show standard deviations. Statistical analyses were performed by means of one-way ANOVA and Dunnett's multiple-comparisons test. Significant differences of samples against the ED sample are shown; $^{**}P < 0.01$, $^{*}P < 0.05$.

to moderate light (50 μmol photon m^{-2} sec^{-1}) occurred in the *sta6* mutant and matched DGAT3 induction. Neither of the other two enzymes evaluated (DGAT1 and PDAT) could explain the boost of TAGs in moderate light in the *sta6* mutant. The evaluation of those two enzymes was not circumstantial. PDAT is targeted to the chloroplast in *C. reinhardtii* and can synthesize TAGs from several substrates (Yoon *et al.*, 2012). DGAT1, although frequently assumed to be localized to the ER, has a predicted chloroplast transit peptide and could be anchored to the chloroplast envelope (Bagnato *et al.*, 2017b). Hence, although we cannot rule out that either post-translational activation or the expression of other enzymes (e.g. DGAT2 and phytyl ester synthases) participate in moderate light-activated TAG production, the strong agreement between TAG levels and DGAT3 expression provides the appealing possibility that the accumulation of TAGs in response to limiting light is catalyzed by DGAT3. Unfortunately, there are no *dgat3* mutants available in the Chlamydomonas Library Project (CLiP). As mRNA expression patterns suggest that DGAT3 is likely to have housekeeping functions, obtaining a reliable mutant might not be a minor task as *dgat3* knockout might result in lethality. In general, the generation of stable nuclear gene knockouts and knockdowns is difficult in *C. reinhardtii* concerning the integration of the transgene by random insertion and the silencing and instability of the transgenes (Neupert *et al.*, 2009; Neupert *et al.*, 2020). In addition, the TAG synthesis pathway is not easy to analyze genetically in organisms such as *C. reinhardtii*, as they feature several enzymes and isoforms that generate the same product and might have overlapping roles. CRISPR-Cas9 has recently started to show promise in *Chlamydomonas* (Greiner *et al.*, 2017; Park *et al.*, 2020), although the successful cases are neither numerous nor widespread. Future work will be aimed at following a CRISPR-Cas9-based reverse genetics approach to interrogate the function of the *dgat3* gene.

The effect of high light, although related, has significant differences with light activation. In high light, it has been demonstrated that the rate of photosynthesis becomes saturated, but light in excess is still absorbed and can damage the photosystems and other macromolecules within the

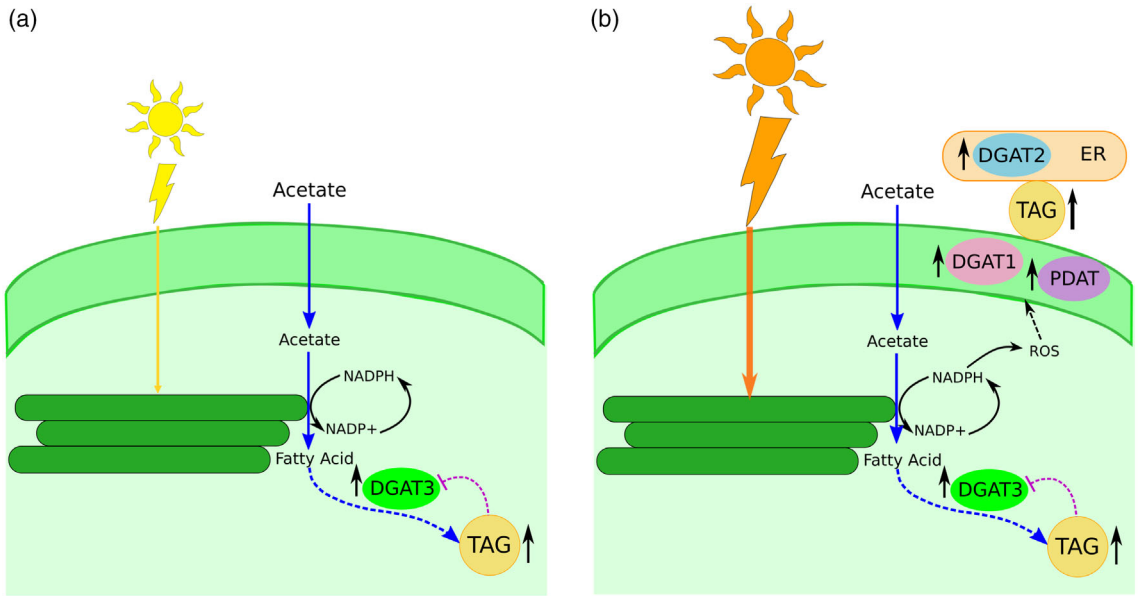

Figure 7. Schematic model of light-induced TAG accumulation in *Chlamydomonas reinhardtii*. (a) In the presence of acetate, when cells are transferred from dark to moderate light conditions, a pulse increase in DGAT3 expression occurs (upwards black arrow by DGAT3). We hypothesize that reducing power provided by light and organic carbon supplied in the form of acetate are directed, as part of the regulation of this enzyme, towards the synthesis of TAGs in the chloroplast, which also increase with moderate light (upwards black arrow by TAG). When the levels of TAGs reach a certain level, we propose that a regulatory loop inhibits further DGAT3 expression and TAG synthesis (purple dashed line). This mechanism could prevent light activation in cc-125 cells that come from a hypoxic dark period and have, thus, elevated pre-existing TAG levels. Although we propose that all these effects are related to the DGAT activity of DGAT3, our experiments cannot rule out an effect of light on TAG turnover. (b) When cells are transferred to high light, we hypothesize that DGAT3-mediated TAG accumulation is not enough to harness the electron excess provided by light. Hence, the expression of stress/reactive oxygen species (ROS)-related enzymes, such as DGAT1 (this work), PDAT and DGAT2 (Chouhan *et al.*, 2022), is activated. DGAT1 is shown on the chloroplast envelope, but it could also be in the endoplasmic reticulum (ER). We cannot conclude from our results whether the differences in the response of DGAT3 to moderate and high light are qualitative or quantitative, or whether DGAT3 expression is induced at higher or lower light irradiances than those evaluated in this work, but we propose that the responses shown in (b) are activated gradually as more photons that are absorbed cannot be stored by the mechanisms in (a). In addition, although the response to moderate light might only involve the chloroplast, the response to high light might occur in both the plastid and the ER/cytosol, as proposed previously (Chouhan *et al.*, 2022; Goold *et al.*, 2016). Dashed lines correspond to processes yet to be fully demonstrated. Only the synthesis of TAGs is shown, without addressing the location of their final storage.

cell (Niyogi, 1999). Hence, the response to high light is probably a combination of light activation and the stimulation of photoprotective mechanisms. In our case, TAG accumulation in wild-type cc-125 cells under high light (200 μmol photon m^{-2} sec^{-1}) was accompanied by an upregulation of both *dgat3* and *dgat1* mRNAs. Even though not all enzymes that can synthesize TAGs have been evaluated in our high-light experiments, one could hypothesize that a more general response to stress is activated in these conditions compared with moderate light. Recently, it was demonstrated that high light induces ROS, which leads to TAG accumulation, in agreement with an increase in DGAT2A and PDAT (Chouhan *et al.*, 2022). All these results suggest that light activation and light stress operate via related, but not necessarily identical, pathways. We propose that whereas moderate light might only induce DGAT3 expression and TAG accumulation in the chloroplast (Figure 7a), high light might also activate the expression of other enzymes that participate either in the chloroplast or the ER, as shown in Figure 7(b) and as also proposed previously (Chouhan *et al.*, 2022; Goold *et al.*, 2016). In addition, although DGAT3 expression might be a target of the light signaling transduction cascade, other enzymes involved in TAG synthesis might be targets of stress/ROS signaling cascades (Figure 7a,b). It is noteworthy that, in both moderate light and high light, the increase in *dgat3* mRNAs and TAG levels occurred as a pulse shortly after transferring the cells to light, consistent with light induction, as has been shown for other targets (Beligni *et al.*, 2004; Gray *et al.*, 2003; Idoine *et al.*, 2014; Salvador *et al.*, 1993). *dgat3* mRNAs were previously shown to also respond to nitrogen deprivation, but this occurred only after long periods of imposing this stress (Boyle *et al.*, 2012; Goodenough *et al.*, 2014; Liu *et al.*, 2016). In the same nitrogen-depleted conditions, DGAT1, PDAT and a few of the DGAT2 isoforms had a more rapid response. Altogether, these results suggest that DGAT1, DGAT2 and PDAT are mostly related to stress, as already proposed, whereas DGAT3 expression might be mainly regulated by light and, perhaps indirectly or circumstantially, moderately responsive to sources of stress such as nitrogen deprivation.

The idea that algae accumulate TAGs as a sink for excess photosynthetic energy and reductant in order to prevent photochemical damage was proposed long ago (Roessler, 1990). In this widely accepted hypothesis (Du & Benning, 2016; Hu *et al.*, 2008; Klok *et al.*, 2014; Li *et al.*, 2012; Solovchenko, 2012), photosynthetic carbon and energy assimilation that can no longer be directed to growth results in the storage of excess reduced carbon (overflow products), both in the form of starch and TAGs. In this scenario, the differences in the response of DGAT3 and TAGs to light between the wild type and the *sta6* strains could be explained by the fact that *sta6* cells cannot synthesize starch and have, hence, an increased pressure for the storage of reduced carbon in the form of TAGs. In this work, we provide evidence that reveals more of the differences between the two types of metabolism.

The TAG quantification showed that in wild-type cells the content of these molecules increased in dark-grown batch cultures and remained high until the end of this period, whereas *sta6* cells had low levels of TAGs at the end of the dark period. As Hemschemeier *et al.* (2013) previously reported, TAGs accumulate in *Chlamydomonas* during periods of extended darkness (24 h) in TAP media, through the reduction of oxygen concentration in batch cultures. In our experiments, wild-type cells incubated in the dark most likely generated energy and reducing power from acetate consumption and starch degradation, with TAG levels rising as a result of hypoxia. In contrast, in *sta6* cells the effect of oxygen reduction on TAG accumulation was evidently counteracted by the need to catabolize TAGs for energy and reducing power in the dark. We propose that the differences in light induction between wild-type and *sta6* cells are related to this. After a 16-h period of darkness, neither DGAT3 expression nor TAGs increased upon transferring wild-type cells to light, and we hypothesize that this is related to the high levels of TAGs at the end of the dark period, as the situation changed when darkness was replaced by low light. At the end of a 16 h period of low light the levels of TAGs were low, close to the levels found in the *sta6* strain at the end of the dark period. In this condition, a pulse increase in DGAT3 and TAGs could be observed after shifting the cells to high light, evidencing that DGAT3 and TAGs do respond to light in the wild type. More broadly, our results suggest that light-induced DGAT3 expression and hence TAG accumulation are tied to the pre-existing levels of TAGs. In other words, our model suggests that DGAT3 expression might be subjected to negative feedback inhibition by the end-product TAG (Figure 7). The existence of regulatory loops for TAG biosynthesis in *C. reinhardtii* has already been proposed (Liu *et al.*, 2016). As the over-accumulation of TAGs could lead to cell obesity, growth arrest and cell death, at least during nitrogen deprivation (Goodson *et al.*, 2011), maintaining moderate TAG levels could ensure that the cell can properly store overflow products in a sustainable manner during the growth phase.

It was previously reported that the production of TAGs that occurs under nitrogen deprivation was dependent on exogenous acetate for both *C. reinhardtii* strains *cw15* and *sta6* (Goodenough *et al.*, 2014; Goodson *et al.*, 2011). In this work, the increase in TAGs and DGAT3 levels also depended on the presence of acetate after transferring *sta6* cells from dark to light. In minimal media, *dgat3* mRNA levels markedly decreased in the light, whereas TAG levels remained relatively stable for the first 12 h into the light period and decreased moderately at 24 h. These results extend the observations presented above and suggest that DGAT3 regulation, and eventually TAG synthesis, are at a crossroads between the provision of reducing power by light and carbon supply. The sequence features of DGAT3 are ideal for this type of control. The presence of a 2Fe–2S cluster-binding domain indicates that this protein could accept electrons, directly or indirectly, from the photosynthetic machinery. We could hypothesize that, as part of DGAT3 regulation, these electrons are further funneled towards the synthesis of fatty acids and their acylation onto molecules of DAG (Bagnato *et al.*, 2017b). In this scenario, it is not surprising that the expression of this enzyme is regulated by the two key components of this process: light and carbon.

Although we propose that DGAT3 could synthesize TAGs in the chloroplast, we cannot conclude the final destination of those TAGs from our results. Chloroplast TAGs have been connected to chloroplast lipid droplets (LDs) (Goodenough *et al.*, 2014; Goodson *et al.*, 2011; Goold *et al.*, 2016), but the existence of chloroplast LDs has recently been questioned (Moriyama *et al.*, 2018). Beyond this controversy, several reports have proposed the appealing idea that a direct metabolic flow occurs between the chloroplast envelope and cytosolic LDs, without the essential intervention of the ER (Goodenough *et al.*, 2014; Liu & Benning, 2013; Moriyama *et al.*, 2018). In addition, chloroplast TAGs could be stored into plastoglobules, lipo-protein structures intimately related to the thylakoid membranes that contain TAGs, among other lipophilic compounds (Steinmüller & Tevini, 1985; Tevini & Steinmüller, 1985). If we consider all these possibilities, DGAT3-dependent TAG synthesis could result in the accumulation of TAGs stored in either plastoglobules or LDs, with the LDs found in either the chloroplast or the cytosol. Future research will surely shed light onto the participation of this unique enzyme in the complex TAG metabolism of green algae.

EXPERIMENTAL PROCEDURES

Chlamydomonas reinhardtii strains and culture conditions

The *C. reinhardtii* wild-type strain cc-125 (*137c, mt+ nit1 nit2*), the cell wall-less strain cc-5155 (*mt+ cw15*) and the cell wall-less,

starch-deficient strain cc-4348 (*mt+ sta6-1*), which contains a deletion of the gene encoding an ADP-glucose pyrophosphorylase subunit and, hence, is incapable of starch formation (Zabawinski *et al.*, 2001), were obtained from the Chlamydomonas Resource Center (https://www.chlamycollection.org). Cells were maintained on TAP (Gorman & Levine, 1965) agar plates. Prior to experiments, cells were inoculated at 10^4 cells ml^{-1} in 100-ml Erlenmeyer flasks containing either liquid TAP or Tris-minimal media (Gorman & Levine, 1965) and grown on a rotary shaker at 23°C under continuous white light (6400 K) at 50 μmol photons m^{-2} sec^{-1}. TAP and Tris-minimal media have identical recipes, with the exception that TAP contains 18.3 mM acetate, whereas Tris-minimal is acetate-free. All experiments were started when cell densities were approximately 3×10^6 cells ml^{-1}. Unless specified, in dark–light experiments the cells were transferred to either dark (D) or low light (LL; 20 μmol photons m^{-2} sec^{-1}) conditions for 16 h. Next, cultures were transferred to light of either 50 or 200 μmol photons m^{-2} sec^{-1} (high light). Samples were taken at 1, 6, 12 and 24 h into the light period. As we wished to analyze the effect of light on mRNA and lipid accumulation, the cultures were grown in batch mode until the end of the dark period, but were switched to semi-continuous mode after transferring them to the light, in order to maintain constant cell densities and to avoid any effect of differential cell shading between samples. Previously (Coragliotti *et al.*, 2011), we had achieved this by centrifuging cells from all time points and resuspending them in fresh TAP to avoid any possible effect of nutrients coming from different volumes of fresh medium between samples. However, we modified this procedure as it was recently reported that centrifugation induces lipid production (Kato *et al.*, 2019). The modified protocol involved adding, every hour, the volume of fresh medium necessary to revert the cell density to the value at the end of the dark period, which we had previously determined that did not impact the accumulation of the selected target molecules at the times points analyzed (unpublished results). In addition to the maintenance of cell densities, each sample harvested accounted for 10% or less of the total culture volume, in order to avoid drastic changes in culture volume that could affect light penetration. At the end of the experiments, cells were harvested by centrifugation at 2000 ***g*** for 10 min, supernatants were discarded and pellets were flash-frozen in liquid N_2 and stored at −80°C until further use. At least three independent experiments were performed for each type of experimental design.

Chloroplast isolation

Chloroplasts were isolated according to the original protocols described by Belknap (1983) and subsequent modifications described by Goldschmidt-Clermont *et al.* (1989) and Barnes *et al.* (2004). Two cell wall-less strains (cc-5155 and cc-4348) were used; results for both are included as both strains yielded good-quality chloroplasts. Briefly, cells were harvested at 2×10^6 cells ml^{-1}, pelleted at 1000 ***g*** for 10 min and resuspended in chloroplast isolation buffer (0.3 M sorbitol, 5 mM $MgCl_2$, 5 mM EGTA, 5 mM EDTA, 20 mM Hepes-KOH, pH 8.0, 40 mM $NaHCO_3$). Cells were re-pelleted and washed in chloroplast isolation buffer two more times. The final suspension was pipetted into an ice-cold N_2 decompression chamber (model 4639; Parr Instrument Company, https://www.parrinst.com). The chamber was pressurized at 1034 kPa for 2 min and de-pressurized at about 3 ml min^{-1}. The cells collected at the release tube were loaded onto a 20/45/65% volumetric three-step Percoll gradient. In such a gradient, intact cells will sediment at the bottom of the tube, whereas intact chloroplasts will sediment at the interphase between the 45% and 65% layers, and cell debris, cell contents and lower density extraplastidic fractions will sediment in or on top of the 20% layer. Percoll step solutions were prepared from a 95% Percoll stock solution (95% (v/v) Percoll, 3% (w/v) PEG 6000, 1% (w/v) Ficoll and 1 % (w/v) BSA) diluted into a gradient mixture (25 mM Hepes-KOH pH 8.0, 10 mM EDTA, 5% sorbitol). Gradients were centrifuged in a Sorvall HB-6 swinging bucket rotor at 6000 ***g*** for 20 min at 4°C (with the brake off) (ThermoFisher Scientific, https://www.thermofisher.com). Intact chloroplasts were carefully pipetted from the interphase, washed twice in chloroplast isolation buffer and resuspended in total protein lysis buffer for further analysis.

RNA isolation and RT-qPCR analyses

The Minimum Information for Publication of Quantitative Real-Time PCR Experiments (MIQE) guidelines (Bustin *et al.*, 2009) were followed for experimental design, sample manipulation and data analyses. RNAs were isolated as described previously (Coragliotti *et al.*, 2011) with some modifications. The volumes equivalent to 10^7 cells were harvested per sample and lysis was performed in a 1-ml final volume of 70 mM Tris-HCl, pH 8, 200 mM NaCl, 20 mM EDTA, pH 8 and 2.7% SDS at room temperature (19–22°C) for 30 min. Homogenates were extracted twice with phenol:chloroform:isoamyl alcohol (25:24:1). The upper aqueous phases were precipitated with one volume of isopropyl alcohol overnight at −20°C. Pellets were washed with consecutive 70% and 100% ethanol washes and resuspended in diethyl pyrocarbonate (DEPC)-treated H_2O once dry. RNAs were quantified in a spectrophotometer (ThermoScientific™ NanoDrop™ One^C Microvolume UV-Vis Spectrophotometer; ThermoFisher Scientific) by determining the Abs_{260nm} and purity was estimated with the Abs_{260}/Abs_{280} and the Abs_{260}/Abs_{320} ratios: only samples with values of approximately 2.0 and 1.34, respectively, were used. In addition, RNA integrity was visualized in 0.9% agarose gels stained with Sybr™ Safe (cat. no. S33102; ThermoFisher Scientific). One microgram of total RNAs from each sample was treated with DNAse (cat. no. EN0521; ThermoFisher Scientific) and used for the synthesis of first-strand cDNAs using MMLV (cat. no. 28025013; ThermoFisher Scientific), with both procedures performed according to the manufacturers' instructions. Copy DNAs were stored at −20°C until further use. For RT-qPCR, *dgat3*, *dgat1*, *pdat*, *gblp* and *actin* mRNAs were analyzed. Details on GenBank accession numbers, oligo sequences and length and position of the amplicons on the coding sequence of the mRNAs are shown in Table S4. The optimal temperature and dynamic range of each pair of oligos for each type of experiment were determined. We worked within template concentrations in which acceptable linearity ($R^2 \geq 0.980$) and efficiencies were observed. In addition, only comparisons between genes with efficiencies differing by less than 10% were made (all between 100% and 109% efficiencies). SYBR-Green-based technology was used for RT-qPCR reactions; mixtures were 2 μl of diluted template and 8 μl of FastStart Universal SYBR Green Master (Rox) (cat. no. 04913914001; Sigma-Aldrich, https://www.sigmaaldrich.com). Reactions were set in technical duplicates or triplicates in MicroAmp® Fast Optical 48-well 0.1-ml reaction plates (cat. no. 4375816, Applied Biosystems; ThermoFisher Scientific), covered with 48-well optical adhesive film (cat. no. 4375323, Applied Biosystems; ThermoFisher Scientific) and run in an Applied Biosystems StepOne™ Real-Time PCR System with the following program: holding stage, 95°C for 10 min; cycling stage, 40 cycles of 95°C for 15 sec (melting) and 60°C for 1 min (annealing and extension), with an additional cycle for the determination of melting curves. Only conditions in which the reaction melting curve showed a single peak were analyzed; single amplicons were confirmed in agarose gels for selected samples. Data were analyzed using LINREGPCR (Ruijter *et al.*, 2014)

(Tables S1 and S2) to determine baselines and calculate individual PCR efficiencies for each sample. Starting concentrations for each sample, expressed in arbitrary fluorescence units (N0s) were used to calculate technical averages and to normalize target genes to reference genes and experimental conditions to control conditions.

Immunofluorescence staining and confocal microscopy

Immunofluorescence staining assays were performed as previously described (Uniacke *et al.*, 2011). We used the cell wall-less strains cc-5155 and cc-4348, as this technique is not very amenable to cell-walled strains. Nevertheless, we only show the results of cc-5155 because the cc-4348 strain did not yield nice, intact cells after the procedure. Briefly, cell aliquots were harvested at 1×10^6 cells ml^{-1} and dispensed on poly-L-lysine-coated microscope slides (Sigma-Aldrich). Cells were fixed, bleached and permeabilized with 4% formaldehyde, 100% cold methanol and 2% (v/v) Triton X-100. The addition of methanol upon fixation was done in order to avoid interference from chlorophyll autofluorescence, as described by Uniacke *et al.* (2011). Slides were blocked with 0.1% (w/v) bovine serum albumin (BSA), and then incubated with DGAT3 anti-serum (1:100 dilution) for 75 min. Immunofluorescence staining was performed by incubating the slides with goat anti-rabbit IgG coupled to FITC (Abcam, https://www.abcam.com) for 45 min (1:500 dilution). In order to preserve the fluorescent signal, slides were covered with ProLong Gold Anti-fade reagent (ThermoFisher Scientific). Microscopic analysis of immunofluorescence-stained sections was performed using a Nikon C1 confocal laser scanning microscope (Nikon, https://www.nikon.com). All images were acquired with a Super Fluor 40.0×/1.30/0.22 oil spring-loaded immersion lens. FITC-coupled antibodies were excited at 488 nm and detected at 515–530 nm. The post-processing of images was carried out with the aid of EZ-C1 FREEVIEWER 3.2.

Protein extraction and Western blot analyses

Chlamydomonas reinhardtii proteins were extracted in 50 mM Tris-HCl, pH 8, 1 mM EDTA, 100 mM NaCl, 1% SDS, 1 mM PMSF, 0.5 mM Leupeptin. Protein concentration in homogenates was determined with the bicinchoninic acid reagent using a BSA standard curve. Samples were heated for 3 min at 95°C in 60 mM Tris-HCl, pH 6.8, 12.5 mM EDTA, 2% SDS, 10% glycerol, 1% 2-mercaptoethanol and 0.02% bromophenol blue and separated in 12% SDS-polyacrylamide gels. PageRuler™ Plus pre-stained protein ladder (cat. no. 26619; Thermo Fisher Scientific) was used as the size standard. Gels were either stained with 0.25% Coomassie brilliant blue R-250 or transferred onto nitrocellulose for Western blot analyses. Blots were blocked in 1X Tris-buffered saline with Tween 20 (TSBT) with 5% skimmed milk and incubated with primary antibodies overnight at 4°C on a rotary shaker. The primary antibodies used were: anti-*C. reinhardtii* DGAT3 (1:500 dilution of rabbit polyclonal antisera) (Bagnato *et al.*, 2017b), anti-*C. reinhardtii* PETs (1:1000 dilution of rabbit polyclonal antisera) (Beligni *et al.*, 2004) and mouse monoclonal anti-*Drosophila* β-tubulin (E7 antibody, used at 0.5 μg ml^{-1}, obtained from the Developmental Studies Hybridoma Bank (DSHB), https://dshb.biology.uiowa.edu). E7 was deposited to the DSHB by M. Klymkowsky (DSHB Hybridoma Product E7). The quality and specificity of the anti-DGAT3 antisera had been determined previously (Bagnato *et al.*, 2017b). Blots were washed in 1X TBST and the corresponding secondary antibodies coupled to alkaline phosphatase were incubated at a 1:15 000 dilution for 1 h at room temperature. Blots were developed using nitroblue tetrazolium and 5-bromo-4-chloro-3-indolyl phosphate (Sigma-Aldrich).

Lipid extraction and thin layer chromatography

Lipid extraction was performed according to the method described by Bligh and Dyer (1959). Briefly, cells were resuspended in 3.8 ml of chloroform:methanol:H_2O (1:2:0.8), vortexed for 20 sec and incubated at room temperature for 1 h, with occasional vortexing. Total lipid extraction was evidenced by the white color of the protein solid phase, which indicated that chlorophyll was completely partitioned to the chloroform phase. For phase partitioning, 1 ml of chloroform and 1 ml of H_2O were added and the tubes were centrifuged at 11 000 ***g*** for 2 min at 4°C. The lower chloroform phase was transferred to another tube and extracts were dried under nitrogen stream. Dried extracts were resuspended in a known volume of chloroform and spotted on 500-μm silica gel G-60 thin layer chromatography (TLC) 20 × 15 cm glass plates under nitrogen stream. A mixture of *n*-hexane:diethyl ether:acetic acid (80:20:1 v/v) was used as the running solvent system to separate the TAGs. Plates were run until the solvent front was 1 cm from the top of the plates (approx. 40 min) and dried under nitrogen stream. Lipid bands were located under ultraviolet light after spraying the TLC plates with 2,7-dichlorofluorescein in methanol and exposing them to ammonia vapor. Lipid classes were identified by comparison with standards spotted alongside the samples. Olive oil was used as a standard of TAGs. Oleic acid was kindly provided by Materia Hnos SACIF for use as the free fatty acid standard (product code MATSOL 101 OD; MATERIA, https://www.materiaoleochemicals.com). TAGs were eluted from the silica with chloroform:methanol:water (5,5:1, v/v) and partitioned by the addition of 0.8 volumes of water to recover them in the organic phase. These purified fractions were used to determine the total quantity of TAG per condition using an accurate enzymatic assay based on the GPO-PAP method (Sullivan *et al.*, 1985) (TG Color; Wiener Lab, https://www.wiener-lab.com.ar), used elsewhere (Sánchez Campos *et al.*, 2018), according to the manufacturer's instructions. Each aliquot was dried and resuspended in isopropyl alcohol and vigorously mixed for 1 min. In this procedure, 1 ml of working reagent was combined with 100 μl of isopropyl alcohol extract and incubated at room temperature (25°C) for 30 min. The absorbance was measured in a spectrophotometer at 505 nm and compared with a glycerol standard curve.

Data and statistical analyses

Graphs were created in RSTUDIO, using the DPLYRand GGPLOT2packages (RStudio Team, 2020). For a better visualization of changes induced by light, RT-qPCR graphs were made using fold changes between the light conditions and the corresponding ED or ELL conditions. For qPCR statistical analyses, dN0 values were used. These values are equivalent to dCt values but are corrected by LINREGPCR(Ruijter *et al.*, 2014) for individual sample PCR efficiencies. Correlation between the data from each experiment was evaluated a using Pearson's test. Residuals were calculated and used to test for normal distribution (https://home.ubalt.edu/ntsbarsh/Businessstat/otherapplets/Regression.htm). In the absence of evidence against normal distribution, one-way analysis of variance (ANOVA)was performed in RSTUDIO. Significant differences between light conditions and the corresponding controls (ED or ELL) were evaluated using the post-hoc Dunnet's test, using the RSTUDIO DESCTOOLSpackage. A two-sided alternative hypothesis was used. Significant differences at P values of <0.001, 0.01, 0.05 and 0.1 were reported. All the results of statistical analyses are shown in Table S3.

ACKNOWLEDGEMENTS

We thank Materia Hnos SACIF, Mar del Plata, Argentina for their kind donation of oleic acid. This work was supported by grants to MVB from the Argentinean Consejo Nacional de Investigaciones Científicas y Tecnológicas (CONICET-PIP 11420110100090) and from Agencia Nacional de Promoción Científica y Tecnológica (ANPCyT, PICT-2013-2122). MVB, CB, GG, LP and LM are CONICET Researchers; DS is a CONICET post-doctoral fellow.

AUTHOR CONTRIBUTIONS

MMC and GG took part in algal experiments, in experimental design and in TLC analyses. MMC took part in TAG quantification; GG took part in immunofluorescence staining. DS took part in algal culture and Western blot analyses. LM took part in qPCR analyses. CB and MVB conceived and discussed the main ideas of the article. LAP took part in visualization and editing of the immunofluorescence images. MVB took part in algal experiments and qPCR and Western blot analyses, experimental design, data interpretation and manuscript writing. All authors reviewed and approved the final version for publication.

CONFLICT OF INTEREST

The authors declare that they have no conflicts of interest associated with this work.

DATA AVAILABILITY STATEMENT

All relevant data can be found within the manuscript and its supporting materials.

SUPPORTING INFORMATION

Additional Supporting Information may be found in the online version of this article.

Table S1. Raw qPCR data.

Table S2. Downstream qPCR analyses.

Table S3. Statistical analyses.

Table S4. qPCR oligonucleotides and amplicons.

Figure S1. TAGs accumulate in dark hypoxic *C. reinhardtii* cc-125 cells.

Figure S2. DGAT3 expression in cc-5155 cells transferred from dark to moderate light.

REFERENCES

Allen, J.W., Tevatia, R., Demirel, Y., DiRusso, C.C. & Black, P.N. (2018) Induction of oil accumulation by heat stress is metabolically distinct from N stress in the green microalgae *Coccomyxa subellipsoidea* C169. *PLoS One*, **13**, 1–20.

Aymé, L., Arragain, S., Canonge, M. *et al.* (2018) *Arabidopsis thaliana* DGAT3 is a [2Fe-2S] protein involved in TAG biosynthesis. *Scientific Reports*, **8**, 17254.

Bagnato, C., Prados, M.B., Franchini, G.R., Scaglia, N., Miranda, S.E. & Beligni, M.V. (2017b) Analysis of triglyceride synthesis unveils a green algal soluble diacylglycerol acyltransferase and provides clues to potential enzymatic components of the chloroplast pathway. *BMC Genomics*, **18**, 223.

Bagnato, C., Ten Have, A., Prados, M.B. & Beligni, M.V. (2017a) Computational functional analysis of lipid metabolic enzymes. *Methods in Molecular Biology*, **1609**, 195–216.

Banerjee, A., Maiti, S.K., Guria, C. & Banerjee, C. (2017) Metabolic pathways for lipid synthesis under nitrogen stress in *Chlamydomonas* and *Nannochloropsis*. *Biotechnology Letters*, **39**, 1–11.

Banerjee, C., Dubey, K.K. & Shukla, P. (2016) Metabolic engineering of microalgal based biofuel production: prospects and challenges. *Frontiers in Microbiology*, **7**, 432.

Barnes, D., Cohen, A., Bruick, R.K., Kantardjieff, K., Fowler, S., Efuet, E. *et al.* (2004) Identification and Characterization of a Novel RNA Binding Protein That Associates with the 5′-Untranslated Region of the Chloroplast psbA mRNA. *Biochemistry*, **43**, 8541–8550.

Beligni, M.V., Yamaguchi, K. & Mayfield, S.P. (2004) Chloroplast elongation factor Ts pro-protein is an evolutionarily conserved fusion with the S1 domain-containing Plastid-Specific Ribosomal Protein-7. *Plant Cell*, **16**, 3357–3369.

Belknap, W.R. (1983) Partial purification of intact chloroplasts from Chlamydomonas reinhardtii. *Plant Physiology*, **72**, 1130–1132.

Bhatt-Wessel, B., Jordan, T.W., Miller, J.H. & Peng, L. (2018) Role of DGAT enzymes in triacylglycerol metabolism. *Archives of Biochemistry and Biophysics*, **655**, 1–11.

Björkman, O. & Demmig, B. (1987) Photon yield of O_2 evolution and chlorophyll fluorescence characteristics at 77 K among vascular plants of diverse origins. *Planta*, **170**, 489–504.

Blaby, I.K., Glaesener, A.G., Mettler, T. *et al.* (2013) Systems-level analysis of nitrogen starvation-induced modifications of carbon metabolism in a *Chlamydomonas reinhardtii* starchless mutant. *Plant Cell*, **25**, 4305–4323.

Bligh, E.G. & Dyer, W.J. (1959) A rapid method of total lipid extraction and purification. *Canadian Journal of Biochemistry and Physiology*, **37**, 911–917.

Boyle, N.R., Page, M.D., Liu, B. *et al.* (2012) Three acyltransferases and nitrogen-responsive regulator are implicated in nitrogen starvation-induced triacylglycerol accumulation in *Chlamydomonas*. *The Journal of Biological Chemistry*, **287**, 15811–15825.

Bustin, S.A., Benes, V., Garson, J.A. *et al.* (2009) The MIQE guidelines: minimum information for publication of quantitative real-time PCR experiments. *Clinical Chemistry*, **55**, 611–622.

Cao, H. (2011) Structure-function analysis of diacylglycerol acyltransferase sequences from 70 organisms. *BMC Research Notes*, **4**, 249.

Cao, H., Shockey, J.M., Klasson, K.T., Chapital, D.C., Mason, C.B. & Scheffler, B.E. (2013) Developmental regulation of diacylglycerol acyltransferase family gene expression in tung tree tissues. *PLoS One*, **8**, e76946.

Chen, C.-X., Sun, Z., Cao, H.-S., Fang, F.-L., Ouyang, L.-L. & Zhou, Z.-G. (2015) Identification and characterization of three genes encoding acyl-CoA: diacylglycerol acyltransferase (DGAT) from the microalga *Myrmecia incisa* Reisigl. *Algal Research*, **12**, 280–288.

Chi, X., Hu, R., Zhang, X. *et al.* (2014) Cloning and functional analysis of three diacylglycerol acyltransferase genes from peanut (*Arachis hypogaea L.*). *PLoS One*, **9**, e105834.

Chouhan, N., Devadasu, E., Yadav, R.M. & Subramanyam, R. (2022) Autophagy induced accumulation of lipids in pgrl1 and pgr5 of *Chlamydomonas reinhardtii* under high light. *Frontiers in Plant Science*, **12**, 752634.

Coragliotti, A.T., Beligni, M.V., Franklin, S.E. & Mayfield, S.P. (2011) Molecular factors affecting the accumulation of recombinant proteins in the *Chlamydomonas reinhardtii* chloroplast. *Molecular Biotechnology*, **48**, 60–75.

Du, Z.-Y. & Benning, C. (2016) Triacylglycerol accumulation in photosynthetic cells in plants and algae. In: Nakamura, Y. & Li-Beisson, Y. (Eds.) *Lipids in plant and algae development*. Subcellular Biochemistry, Vol **86**. Cham: Springer Cham, pp. 179–205.

Fan, J., Andre, C. & Xu, C. (2011) A chloroplast pathway for the de novo biosynthesis of triacylglycerol in *Chlamydomonas reinhardtii*. *FEBS Letters*, **585**, 1985–1991.

Fukuyama, K. (2004) Structure and function of plant-type ferredoxins. *Photosynthesis Research*, **81**, 289–301.

Goldschmidt-Clermont, M., Malnoë, P. & Rochaix, J. (1989) Preparation of chlamydomonas chloroplasts for the in vitro import of polypeptide precursors. *Plant Physiology*, **89**, 15–18.

Goodenough, U., Blaby, I., Casero, D. *et al.* (2014) The path to triacylglyceride obesity in the sta6 strain of *Chlamydomonas reinhardtii*. *Eukaryotic Cell*, **13**, 591–613.

Goodson, C., Roth, R., Wang, Z.T. & Goodenough, U. (2011) Structural correlates of cytoplasmic and chloroplast lipid body synthesis in

Chlamydomonas reinhardtii and stimulation of lipid body production with acetate boost. *Eukaryotic Cell*, **10**, 1592–1606.

Goold, H.D., Cuiné, S., Légeret, B. *et al.* (2016) Saturating light induces sustained accumulation of oil in plastidal lipid droplets in *Chlamydomonas reinhardtii*. *Plant Physiology*, **171**, 2406–2417.

Gorman, D.S. & Levine, R.P. (1965) Cytochrome f and plastocyanin: their sequence in the photosynthetic electron transport chain of *Chlamydomonas reinhardi*. *Proceedings of the National Academy of Sciences of the United States of America*, **54**, 1665–1669.

Gray, J.C., Sullivan, J.A., Wang, J.H. *et al.* (2003) Coordination of plastid and nuclear gene expression. *Philosophical Transactions of the Royal Society B: Biological Sciences*, **358**, 135–145.

Greiner, A., Kelterborn, S., Evers, H., Kreimer, G., Sizova, I. & Hegemann, P. (2017) Targeting of photoreceptor genes in Chlamydomonas reinhardtii via zinc-finger nucleases and CRISPR/Cas9. *Plant Cell*, **29**, 2498–2518.

Guo, X., Fan, C., Chen, Y., Wang, J., Yin, W., Wang, R.R.C. *et al.* (2017) Identification and characterization of an efficient acyl-CoA: diacylglycerol acyltransferase 1 (DGAT1) gene from the microalga *Chlorella ellipsoidea*. *BMC Plant Biology*, **17**, 48.

Hemschemeier, A., Casero, D., Liu, B., Benning, C., Pellegrini, M., Happe, T. *et al.* (2013) Copper Response Regulator1-dependent and -independent responses of the *Chlamydomonas reinhardtii* transcriptome to dark anoxia. *Plant Cell*, **25**, 3186–3211.

Hernández, M.L., Whitehead, L., He, Z., Gazda, V., Gilday, A., Kozhevnikova, E. *et al.* (2012) A cytosolic acyltransferase contributes to triacylglycerol synthesis in sucrose-rescued *Arabidopsis* seed oil catabolism mutants. *Plant Physiology*, **160**, 215–225.

Hu, Q., Sommerfeld, M., Jarvis, E., Ghirardi, M., Posewitz, M., Seibert, M. *et al.* (2008) Microalgal triacylglycerols as feedstocks for biofuel production: perspectives and advances. *The Plant Journal*, **54**, 621–639.

Idoine, A.D., Boulouis, A., Rupprecht, J. & Bock, R. (2014) The diurnal logic of the expression of the chloroplast genome in *Chlamydomonas reinhardtii* F. Börnke, ed. *PLoS One*, **9**, e108760.

Kato, N., Lum, T., Légeret, B., Li-Beisson, Y. & Ndathe, R. (2019) Centrifugation-induced production of triacylglycerols in *Chlamydomonas reinhardtii*. *Bioresource Technology Reports*, **5**, 326–330.

Klok, A.J., Lamers, P.P., Martens, D.E., Draaisma, R.B. & Wijffels, R.H. (2014) Edible oils from microalgae: insights in TAG accumulation. *Trends in Biotechnology*, **32**, 521–528.

Li, X., Moellering, E.R., Liu, B., Johnny, C., Fedewa, M., Sears, B.B. *et al.* (2012) A galactoglycerolipid lipase is required for triacylglycerol accumulation and survival following nitrogen deprivation in Chlamydomonas reinhardtii. *Plant Cell*, **24**, 4670–4686.

Li-Beisson, Y., Thelen, J.J., Fedosejevs, E. & Harwood, J.L. (2019) The lipid biochemistry of eukaryotic algae. *Progress in Lipid Research*, **74**, 31–68.

Liu, B. & Benning, C. (2013) Lipid metabolism in microalgae distinguishes itself. *Current Opinion in Biotechnology*, **24**, 300–309.

Liu, J., Han, D., Yoon, K., Hu, Q. & Li, Y. (2016) Characterization of type 2 diacylglycerol acyltransferases in *Chlamydomonas reinhardtii* reveals their distinct substrate specificities and functions in triacylglycerol biosynthesis. *The Plant Journal*, **86**, 3–19.

Liu, Q., Siloto, R.M.P., Lehner, R., Stone, S.J. & Weselake, R.J. (2012) Acyl-CoA:diacylglycerol acyltransferase: molecular biology, biochemistry and biotechnology. *Progress in Lipid Research*, **51**, 350–377.

Liu, Q., Siloto, R.M.P., Snyder, C.L. & Weselake, R.J. (2011) Functional and topological analysis of yeast acyl-CoA:diacylglycerol acyltransferase 2, an endoplasmic reticulum enzyme essential for triacylglycerol biosynthesis. *The Journal of Biological Chemistry*, **286**, 13115–13126.

Lopes, J.L.S., Nobre, T.M., Cilli, E.M., Beltramini, L.M., Araújo, A.P.U. & Wallace, B.A. (2014) Deconstructing the DGAT1 enzyme: Binding sites and substrate interactions. *Biochimica et Biophysica Acta - Biomembranes*, **1838**, 3145–3152.

Lung, S.C. & Weselake, R.J. (2006) Diacylglycerol acyltransferase: a key mediator of plant triacylglycerol synthesis. *Lipids*, **41**, 1073–1088.

Martin, G.J.O., Hill, D.R.A., Olmstead, I.L.D. *et al.* (2014) Lipid profile remodeling in response to nitrogen deprivation in the microalgae *Chlorella sp.* (Trebouxiophyceae) and *Nannochloropsis sp.* (Eustigmatophyceae). *PLoS One*, **9**, e103389.

Moriyama, T., Toyoshima, M., Saito, M., Wada, H. & Sato, N. (2018) Revisiting the algal chloroplast lipid droplet: the absence of an entity that is unlikely to exist. *Plant Physiology*, **176**, 1519–1530.

Msanne, J., Xu, D., Konda, A.R., Casas-Mollano, J.A., Awada, T., Cahoon, E.B. *et al.* (2012) Metabolic and gene expression changes triggered by nitrogen deprivation in the photoautotrophically grown microalgae *Chlamydomonas reinhardtii* and *Coccomyxa sp.* C-169. *Phytochemistry*, **75**, 50–59.

Neupert, J., Gallaher, S.D., Lu, Y. *et al.* (2020) An epigenetic gene silencing pathway selectively acting on transgenic DNA in the green alga Chlamydomonas. *Nature Communications*, **11**, 1–17.

Neupert, J., Karcher, D. & Bock, R. (2009) Generation of Chlamydomonas strains that efficiently express nuclear transgenes. *The Plant Journal*, **57**, 1140–1150.

Niyogi, K.K. (1999) Photoprotection revisited: genetic and molecular approaches. *Annual Review of Plant Physiology and Plant Molecular Biology*, **50**, 333–359.

Pal, D., Khozin-Goldberg, I., Cohen, Z. & Boussiba, S. (2011) The effect of light, salinity, and nitrogen availability on lipid production by Nannochloropsis sp. *Applied Microbiology and Biotechnology*, **90**, 1429–1441.

Park, R.V., Asbury, H. & Miller, S.M. (2020) Modification of a Chlamydomonas reinhardtii CRISPR/Cas9 transformation protocol for use with widely available electroporation equipment. *MethodsX*, **7**, 100855.

Rearte, T.A., Vélez, C.G., Beligni, M.V., Figueroa, F.L., Gómez, P.I., Flaig, D. *et al.* (2018) Biological characterization of a strain of *Golenkinia* (Chlorophyceae) with high oil and carotenoid content induced by increased salinity. *Algal Research*, **33**, 218–230.

RStudio Team. (2020) RStudio: Integrated Development Environment for R. Available at: http://www.rstudio.com/.

Roessler, P.G. (1990) Environmental control of glycerolipid metabolism in microalgae: commercial implications and future research directions. *Journal of Phycology*, **26**, 393–399.

Ruijter, J.M., Lorenz, P., Tuomi, J.M., Hecker, M. & van den Hoff, M.J.B. (2014) Fluorescent-increase kinetics of different fluorescent reporters used for qPCR depend on monitoring chemistry, targeted sequence, type of DNA input and PCR efficiency. *Microchimica Acta*, **181**, 1689–1696.

Saha, S., Enugutti, B., Rajakumari, S. & Rajasekharan, R. (2006) Cytosolic triacylglycerol biosynthetic pathway in oilseeds. Molecular cloning and expression of peanut cytosolic diacylglycerol acyltransferase. *Plant Physiology*, **141**, 1533–1543.

Salvador, M.L., Klein, U. & Bogorad, L. (1993) Light-regulated and endogenous fluctuations of chloroplast transcript levels in *Chlamydomonas*. Regulation by transcription and RNA degradation. *The Plant Journal*, **3**, 213–219.

Sánchez Campos, S., Alza, N.P. & Salvador, G.A. (2018) Lipid metabolism alterations in the neuronal response to A53T α-synuclein and Fe-induced injury. *Archives of Biochemistry and Biophysics*, **655**, 43–54.

Sato, N., Moriyama, T., Mori, N. & Toyoshima, M. (2017) Lipid metabolism and potentials of biofuel and high added-value oil production in red algae. *World Journal of Microbiology and Biotechnology*, **33**, 74.

Sharma, K.K., Schuhmann, H. & Schenk, P.M. (2012) High lipid induction in microalgae for biodiesel production. *Energies*, **5**, 1532–1553.

Shockey, J.M., Gidda, S.K., Chapital, D.C., Kuan, J.-C., Dhanoa, P.K., Bland, J.M. *et al.* (2006) Tung tree DGAT1 and DGAT2 have nonredundant functions in triacylglycerol biosynthesis and are localized to different subdomains of the endoplasmic reticulum. *Plant Cell*, **18**, 2294–2313.

Solovchenko, A.E. (2012) Physiological role of neutral lipid accumulation in eukaryotic microalgae under stresses. *Russian Journal of Plant Physiology*, **59**, 167–176.

Steinmüller, D. & Tevini, M. (1985) Composition and function of plastoglobuli – I. Isolation and purification from chloroplasts and chromoplasts. *Planta*, **163**, 201–207.

Stone, S.J., Levin, M.C. & Farese, R.V. (2006) Membrane topology and identification of key functional amino acid residues of murine Acyl-CoA:diacylglycerol acyltransferase-2. *The Journal of Biological Chemistry*, **281**, 40273–40282.

Sullivan, D.R., Kruijswijk, Z., West, C.E., Kohlmeier, M. & Katan, M.B. (1985) Determination of serum triglycerides by an accurate enzymatic method not affected by free glycerol. *Clinical Chemistry*, **31**, 1227–1228.

Takeuchi, K. & Reue, K. (2009) Biochemistry, physiology, and genetics of GPAT, AGPAT, and lipin enzymes in triglyceride synthesis. *American Journal of Physiology - Endocrinology and Metabolism*, **296**, E1195–E1209.

Takeuchi, T. & Benning, C. (2019) Nitrogen-dependent coordination of cell cycle, quiescence and TAG accumulation in *Chlamydomonas*. *Biotechnology for Biofuels*, **12**, 292.

Tevini, M. & Steinmüller, D. (1985) Composition and function of plastoglobuli – II. Lipid composition of leaves and plastoglobuli during beech leaf senescence. *Planta*, **163**, 91–96.

Tsai, C.-H., Zienkiewicz, K., Amstutz, C.L., Brink, B.G., Warakanont, J., Roston, R. *et al.* (2015) Dynamics of protein and polar lipid recruitment during lipid droplet assembly in *Chlamydomonas reinhardtii*. *The Plant Journal*, **83**, 650–660.

Turchetto-Zolet, A.C., Maraschin, F.S., de Morais, G.L., Cagliari, A., Andrade, C.M., Margis-Pinheiro, M. *et al.* (2011) Evolutionary view of acyl-CoA diacylglycerol acyltransferase (DGAT), a key enzyme in neutral lipid biosynthesis. *BMC Evolutionary Biology*, **11**, 263–277.

Uniacke, J., Colón-Ramos, D. & Zerges, W. (2011) FISH and immunofluorescence staining in Chlamydomonas. *Methods in Molecular Biology*, **714**, 15–29.

Weng, L.-C., Pasaribu, B., Ping Lin, I. *et al.* (2014) Nitrogen deprivation induces lipid droplet accumulation and alters fatty acid metabolism in symbiotic dinoflagellates isolated from *Aiptasia pulchella*. *Scientific Reports*, **4**, 41–49.

Xu, C., Andre, C., Fan, J. & Shanklin, J. (2016) Cellular organization of triacylglycerol biosynthesis in microalgae. *Sub-Cellular Biochemistry*, **86**, 207–221.

Xu, Y., Caldo, K.M.P., Pal-Nath, D., Ozga, J., Lemieux, M.J., Weselake, R.J. *et al.* (2018) Properties and biotechnological applications of acyl-CoA:diacylglycerol acyltransferase and phospholipid:diacylglycerol acyltransferase from terrestrial plants and microalgae. *Lipids*, **53**, 663–688.

Yamashita, A., Hayashi, Y., Matsumoto, N., Nemoto-Sasaki, Y., Oka, S., Tanikawa, T. *et al.* (2014) Glycerophosphate/Acylglycerophosphate acyltransferases. *Biology (Basel)*, **3**, 801–830.

Yang, D., Song, D., Kind, T. *et al.* (2015) Lipidomic analysis of *Chlamydomonas reinhardtii* under nitrogen and sulfur deprivation S. N. Witt, ed. *PLoS One*, **10**, e0137948.

Yeh, A.P., Chatelet, C., Soltis, S.M., Kuhn, P., Meyer, J. & Rees, D.C. (2000) Structure of a thioredoxin-like [2Fe-2S] ferredoxin from *Aquifex aeolicus*. *Journal of Molecular Biology*, **300**, 587–595.

Yen, C.L.E., Stone, S.J., Koliwad, S., Harris, C. & Farese, R.V. (2008) DGAT enzymes and triacylglycerol biosynthesis. *Journal of Lipid Research*, **49**, 2283–2301.

Yoon, K., Han, D., Li, Y., Sommerfeld, M. & Hu, Q. (2012) Phospholipid:diacylglycerol acyltransferase is a multifunctional enzyme involved in membrane lipid turnover and degradation while synthesizing triacylglycerol in the unicellular green microalga *Chlamydomonas reinhardtii*. *Plant Cell*, **24**, 3708–3724.

Zabawinski, C., Van den Koornhuyse, N., D'Hulst, C., Schlichting, R., Giersch, C., Delrue, B. *et al.* (2001) Starchless mutants of *Chlamydomonas reinhardtii* lack the small subunit of a heterotetrameric ADP-glucose pyrophosphorylase. *Journal of Bacteriology*, **183**, 1069–1077.

Zu, Y., Di Bernardo, S., Yagi, T. & Hirst, J. (2002) Redox properties of the [2Fe-2S] center in the 24 kDa (NQO_2) subunit of NADH:ubiquinone oxidoreductase (Complex I). *Biochemistry*, **41**, 10056–10069.